

Journal Pre-proof

Twinning, slip and size effect of phase-transforming ferroelectric nanopillars

Zeyuan Zhu, Mostafa Karami, Chenbo Zhang, Xian Chen



PII: S0022-5096(24)00262-X
DOI: <https://doi.org/10.1016/j.jmps.2024.105796>
Reference: MPS 105796

To appear in: *Journal of the Mechanics and Physics of Solids*

Received date: 17 March 2024
Revised date: 2 July 2024
Accepted date: 22 July 2024

Please cite this article as: Z. Zhu, M. Karami, C. Zhang et al., Twinning, slip and size effect of phase-transforming ferroelectric nanopillars. *Journal of the Mechanics and Physics of Solids* (2024), doi: <https://doi.org/10.1016/j.jmps.2024.105796>.

This is a PDF file of an article that has undergone enhancements after acceptance, such as the addition of a cover page and metadata, and formatting for readability, but it is not yet the definitive version of record. This version will undergo additional copyediting, typesetting and review before it is published in its final form, but we are providing this version to give early visibility of the article. Please note that, during the production process, errors may be discovered which could affect the content, and all legal disclaimers that apply to the journal pertain.

© 2024 Elsevier Ltd. All rights are reserved, including those for text and data mining, AI training, and similar technologies.

Twinning, Slip and Size Effect of Phase-Transforming Ferroelectric Nanopillars

Zeyuan Zhu^a, Mostafa Karami^a, Chenbo Zhang^b, Xian Chen^{a,*}

^aDepartment of Mechanical and Aerospace Engineering, Hong Kong University of Science and Technology, Hong Kong
^bMOE Key Laboratory of Advanced Micro-Structured Materials, School of Physics Science and Engineering, Institute for Advanced Study, Tongji University, Shanghai, 200092, China

Abstract

Ferroelectric materials are widely used in energy applications due to their field-driven multiferroic properties. The stress-induced phase transformation plays an important role in the functionality over repeated and consecutive operation cycles, especially at the micro/nanoscales. Here we report a systematic in-situ uniaxial compression tests on cuboidal Barium titanate (BaTiO_3) nanopillars with size varying from 100 nm to 3000 nm, by which we explore the stress-induced transformation and its interplay with plastic deformation. We confirm the superelasticity achieved in pillars by martensitic phase transformation from tetragonal to orthorhombic. There exists a critical size, 330nm, for the yield stress. Above 330nm, martensitic phase transformation aids slip along the plane with a low Schmid factor, in turn, the pseudo-compatible twins form within the shear band. The scaling exponent of size-dependent yield strength is found to be exactly 1. For nanopillars smaller than 330nm, no twins form, only slips with large Schmid factors are activated, and size effect vanishes. All pillars with sizes from 100nm to 300nm achieve the theoretical yield limit around 9GPa. Our experimental results uncover the interplay between twins and slips in BaTiO_3 nanopillars, which pave the way for the optimization of microstructure design of ferroelectric materials for microelectronic applications at small scales.

Keywords: Twinning, Slip, Size effect, Phase-transforming ferroelectrics, In situ nanomechanical test

1. Introduction

Ferroelectric materials provide profound potentials in energy applications [1] such as piezoelectric energy harvesting [2], electrocaloric cooling [3], and pyroelectric energy generators [4, 5]. The performance of these devices relies on the field-driven multiferroic properties, which are sensitive to the symmetries and lattice parameters of the ferroelectric crystals. Barium titanate is a typical phase transforming ferroelectric material with a wide range of applications to electronic devices. Above the Curie temperature (i.e. around

*Corresponding author
Email address: xianchen@ust.hk (Xian Chen)

120°C), it possesses a cubic perovskite structure, which transforms to a ferroelectric tetragonal phase, then to orthorhombic at 5°C finally to rhombohedral phase at -80°C . [6] When the structural phase transformation occurs in the crystal, the ferroic properties of the material undergo an abrupt change, which strongly enhance the energy conversion performance. Regard the device design, the stress-induced phase transformation plays an important role in the functionality over repeated and consecutive operation cycles, especially at the micro/nanoscales [7]. While many studies discuss the effect of mechanical stress on elastic and plastic behaviors [8, 9] and domain switching [10], the stress-induced transformation and interplay between twins and slips are rarely investigated in ferroelectric oxides.

The ferroelectric oxides are generally brittle [11, 12]. Unlike metals, ferroelectric oxides rarely exhibit common slip systems such as (111)[$\bar{1}\bar{1}0$] for face-centered cubic and (110)[$\bar{1}\bar{1}1$] for body-centered cubic. In BaTiO_3 , an easy glide system (110)[$\bar{1}\bar{1}0$] were observed by micro/nanoindentation experiments [13, 14, 15], despite statistically stored dislocations primarily having the Burgers vector along [100] direction, as observed by TEM [16, 17]. In some micromechanical experiments, the slip system (110)[$\bar{1}\bar{1}0$] and its crystallographic equivalencies [12, 18] were activated corresponding to the maximum Schmid factor (i.e. 0.5) under uniaxial pillar compression along [001] orientation. When the loading direction does not favor slip along [$\bar{1}\bar{1}0$] on the (110) plane, other slip systems can be activated at different shear stress levels. However, there are no experiments to support the existences of other slip systems in Barium titanates. In some cases, the compression experiments on [001]-oriented single crystal BaTiO_3 exhibit superelasticity under 50 MPa applied stress [19, 18]. These works claim that the superelasticity was achieved by domain switching rather than phase transition, but accurate experimental justification with quantitative microstructure analysis is not verified under a general orientation away from the easy axis. The crystallographic calculations of transformation strain were not performed to examine whether the superelasticity is due to the phase transformation or the domain switching.

For phase transforming ferroelectric materials, formation of twins and activation of dislocation slips may lead to a complicated deformation mode, consequently, causing new mechanical scaling law at nanoscales. Conventionally, phenomenological analysis concluded that the material gets stronger as the size reduces. In polycrystalline solids, this is interpreted as the Hall-Petch relation [20, 21] that the flow stress is inversely related to the grain size. From continuum mechanics point of view, the yield stress scales up with the reduction of sample size through a power law. The high-order models of strain-gradient plasticity [22, 23, 24] predict that the scaling exponent is equal to 1 by direct minimization of the free energy functional considering uniform strain gradient with a simple shear. However, conventional strain-gradient models often over predicted the exponent α from experimental values, specially in the micro to nanomechanical experimental regime [25, 26, 27, 28]. As the ferroelectric oxides are rigid and brittle, the strain gradient hardening model may predict them more accurately than metals. It is interesting to investigate the scaling law of yield strength for phase-transforming ferroelectrics at small scales.

In this paper, we conduct systematic in-situ uniaxial compression tests on cuboidal BaTiO₃ nanopillars with size varying from 100 nm to 3000 nm, to explore the stress-induced transformation and its interplay with plastic deformation. We investigate the scaling law for bulk and miniature pillars and discover a critical size. Above the critical size, martensitic phase transformation fabricates slip along the plane with a low Schmid factor. Below the critical size, no twins form, and only slips with large Schmid factors are activated. The microstructure of the post-deformed specimen is carefully analyzed by crystallographic theory of martensite. We also precisely measure the strength dependent scaling behaviors under two deformation regimes corresponding to the microstructure observation of fracture mechanisms.

2. Analysis of twins and slips in BaTiO₃ under uniaxial loading

Since the discovery of Barium titanate (BaTiO₃), its crystal structures have been thoroughly characterized at temperatures from -80°C to 200°C by X-ray and neutron diffraction experiments [29, 30, 6]. Here we focus on the formation of twins from tetragonal phase (*P4mm*) to orthorhombic phase (*Amm2*). The symmetry-breaking phase transformation results in two symmetry-related martensitic variants, represented by the transformation stretch tensors \mathbf{U}_1 and \mathbf{U}_2 . During the phase transformation, the (010)_t plane and [101]_t, $[\bar{1}01]_t$ directions of tetragonal lattice transform to the (100)_o plane and [010]_o, [001]_o directions of orthorhombic lattice. The lattice correspondence is indicated in Figure 1(a) and (b). The stretch tensors can be explicitly calculated in terms of lattice parameters as

$$\mathbf{U}_1^2 = \begin{bmatrix} \frac{b_o^2+c_o^2}{4a_t^2} & 0 & \frac{b_o^2-c_o^2}{4a_t c_t} \\ 0 & \frac{a_o^2}{a_t^2} & 0 \\ \frac{b_o^2-c_o^2}{4a_t c_t} & 0 & \frac{b_o^2+c_o^2}{4c_t^2} \end{bmatrix}, \quad \mathbf{U}_2^2 = \begin{bmatrix} \frac{b_o^2+c_o^2}{4a_t^2} & 0 & \frac{c_o^2-b_o^2}{4a_t c_t} \\ 0 & \frac{a_o^2}{a_t^2} & 0 \\ \frac{c_o^2-b_o^2}{4a_t c_t} & 0 & \frac{b_o^2+c_o^2}{4c_t^2} \end{bmatrix}. \quad (1)$$

The lattice parameters were reported as $a_t = 3.997\text{\AA}$, $c_t = 4.0314\text{\AA}$ for tetragonal, and $a_o = 3.9874\text{\AA}$, $b_o = 5.6751\text{\AA}$, $c_o = 5.6901\text{\AA}$ for orthorhombic by Kwei et al. [6]. Figure 1 elaborates the transformation mechanism from tetragonal lattice to orthorhombic lattice. By substituting the lattice parameters, we calculate the eigenvalues of the stretch tensor in (1), as

$$(\lambda_1, \lambda_2, \lambda_3) = (0.9965, 0.9976, 1.0055).$$

The middle eigenvalue $\lambda_2 \neq 1$ suggests that the single orthorhombic variant can not grow directly from the tetragonal lattice through a compatible interface. Twins must form in orthorhombic phase to accommodate the incompatibility. The orthorhombic lattices that are deformed by two variants \mathbf{U}_1 and \mathbf{U}_2 , in Figure 1(b), exhibit a mirror relation crossing the twinning plane $(00\bar{1})_t || (011)_o$. According to the crystallographic theory of martensite, there must exist a conjugate twin with a mirror plane $(100)_t$. The twins with mirror planes $(00\bar{1})_t$ and $(100)_t$ are compound twins. During martensitic transformation, either twin can form based on compatibility conditions [31].

Besides twins, the low index planes such as $(100)_t$, $(\bar{1}\bar{1}0)_t$ and $(11\bar{1})_t$ shown in Figure 1 (c) are possible slip planes for the stretched perovskite BaTiO_3 lattice. Within an atomic stacking period, the areal packing factor can be defined as

$$\rho_{hkl} = \frac{\text{area of all ions in } (hkl) \text{ plane}}{\text{area of } (hkl) \text{ plane}}. \quad (2)$$

As illustrated in Figure 1 (c), direct calculation by (2) gives $\rho_{(\bar{1}\bar{1}0)_t} = 0.77$, $\rho_{(11\bar{1})_t} = 0.74$, and $\rho_{(100)_t} = 0.69$. Although stretching along c_t -axis may slightly distort the lattice from normal perovskite structure, the family of $\{110\}$ corresponds to the closest packed planes in tetragonal BaTiO_3 . The second closest packed plane is $(11\bar{1})_t$, with slightly smaller areal packing factor. We speculate that slips can be activated on both $(\bar{1}\bar{1}0)_t$ and $(11\bar{1})_t$ planes depending on the loading conditions. In Figure 1(c), we plot the slip systems by depicting the slip directions associated with least shearing distances. Among them, $(\bar{1}\bar{1}0)_t[110]_t$, $(\bar{1}\bar{1}0)_t[001]_t$, $(\bar{1}\bar{1}0)_t[11\bar{1}]_t$, $(11\bar{1})_t[1\bar{1}0]_t$ are the feasible slip systems for tetragonal BaTiO_3 , while $(100)_t[010]_t$ is hard to be activated. Many experiments have shown that the slip system $(\bar{1}\bar{1}0)_t[110]_t$ got activated during uniaxial loading along $[001]_t$ direction in single crystal BaTiO_3 [13, 14, 15]. But the activation of other slip systems has not been reported yet.

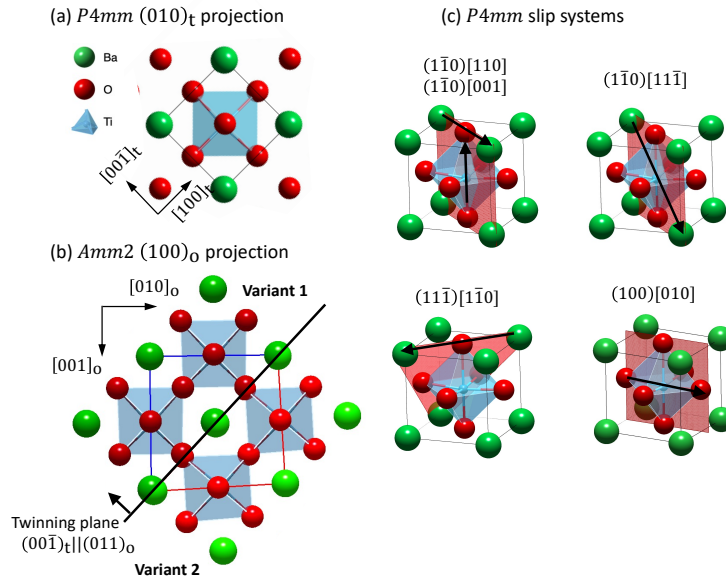


Figure 1: BaTiO_3 crystal structures for tetragonal to orthorhombic symmetries before and after martensitic phase transformation. (a) Tetragonal lattice on $(010)_t$ plane corresponding to (b) two orthorhombic variants on $(100)_o$ plane twinned through $(011)_o$ plane. (c) Possible slip systems in BaTiO_3 tetragonal lattice on planes $(\bar{1}\bar{1}0)$, $(11\bar{1})$ and (100) written in terms of cubic basis.

3. In situ nanomechanical experiment and result

In this section, we investigate the twin formation and slip activation in single-crystal BaTiO₃ nanopillars. Without loss of generality, the nanopillars are fabricated along a direction that deviates from the ferroelectric easy axis.

The BaTiO₃ used in this study is a bulk polycrystalline material, synthesized using the conventional solid-state reaction method [32]. To facilitate nanomechanical testing, we employed a floating zone sintering method to grow coarse, equiaxial grains approximately 100 μm in size. The specifics of the thermal processing and floating zone parameters can be found in Zhang et al. (2023) [33]. Following sintering, the bulk material was sectioned and polished in preparation for both microstructural analysis and mechanical testing. We fabricated cuboidal pillars with side lengths ranging from 3000 nm to 100 nm, maintaining an aspect ratio of approximately 3:1. All cuboidal pillars were milled by using the FEI Helios G4 UX dual-beam focused ion beam (FIB) milling system. Figure 2 (a) shows an overview of the pillar array that locates at the edge of the bulk sample so that the pillar's lateral surface can be seen under the in situ mechanical test. The orientation distribution of the grain is relatively homogeneous, characterized by Electron Backscatter diffraction (EBSD) in Figure 2 (b) and (c). The diffracted Kikuchi lines were analyzed by $P4mm$ symmetry. Figure 2 (d) shows the calculated Kikuchi pattern giving the orientation matrix

$$\mathbf{O}_t = \begin{bmatrix} 0.40592 & 0.91297 & 0.04134 \\ 0.36104 & -0.20175 & 0.91047 \\ 0.83957 & -0.35465 & -0.41151 \end{bmatrix}. \quad (3)$$

The last column of the orientation matrix indicates the pillar's end-surface normal, while the first and second columns refer to the lateral surface frame upon a 45° rotation. Here the pillar orientation is close to the crystallographic direction $[02\bar{1}]_t$, fairly away from any special symmetric axes associated with the oxygen octahedron. It is a sufficiently general orientation to study the interplay between twins and slips in BaTiO₃. Nanopillars with size varying from 100 nm to 3000 nm were fabricated by FIB in the domain with out-of-plane normal near $[02\bar{1}]_t$, tested under uniaxial compression. The stress-strain curves were recorded to reveal the superelasticity and size-dependent strength of BaTiO₃ nanopillars.

3.1. Nanomechanical test for stress-induced phase transformation in BaTiO₃

We used the FemtoTools Nanomechanical Testing system (model FTNMT03, Buchs ZH, Switzerland) under FEI Quanta 250 FEG SEM to conduct the in situ uniaxial nanocompression tests. All loading procedures were carried out at a thermal stable environment at 25°C under the displacement control mode using a 5 μm diamond flat punch. The details of the in situ experimental setup can be found in Karami et al. [34, 35]. The loading direction was aligned with the orientation of all the pillars, i.e. $\mathbf{N} = [02\bar{1}]_t = (0.041, 0.91, -0.411)$. Hereafter we use the cubic basis to present the tensors in all continuum mechanics

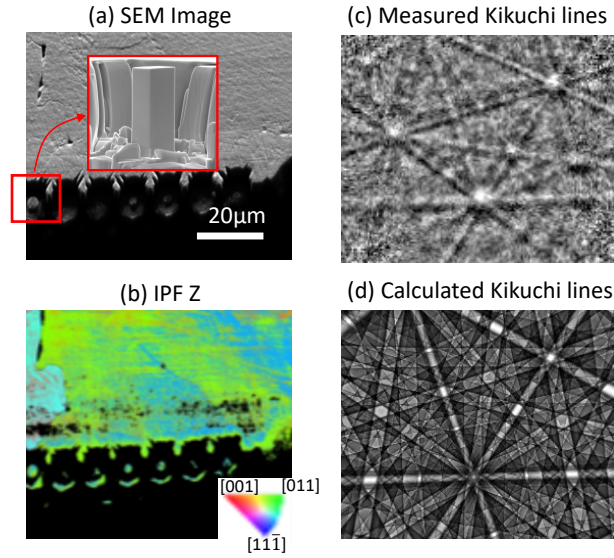


Figure 2: Grain orientation characterized by EBSD. (a) The SEM image showing the grain morphology corresponding to (b) the Inverse Pole Figure (IPF) with Z-axis color map. (c) The measured Kikuchi lines by electron diffraction from the characterized region. (d) Calculated Kikuchi lines by the $P4mm$ symmetry with Z-axis approximately aligned with crystallographic direction $[02\bar{1}]_t$.

calculations. Precise adjustments were made to the positions between the punch and pillar using a 5-axis adjustable stage to ensure optimal alignment. The maximum applied stress was properly chosen to induce the martensitic phase transformation without causing plastic deformation during this experiment. The electron beam was positioned perpendicular to the lateral surface of the pillars for real-time monitoring the deformation. In this experiment, we used the real-time imaging to ensure the compressive force does not cause visual slips in the pillars. The stress is computed as the force per reference cross-sectional area, and strain is calculated as the relative depth change of the pillar with respect to the original length.

As seen from the stress-strain curves in Figure 3, the nanopillars from 130nm to 2800nm exhibit large deformability and reversibility upon loading and unloading processes at a low stress level ($< 400\text{MPa}$). 0.6~1% recoverable strains were characterized by the nanocompression tests for all tested pillars. Compared to ordinary non-transforming ceramics, the measured recoverable strain of BaTiO_3 is magnificent, which suggests that reversible martensitic transformation plays a role in the low-stress loading regime. We observed a clear plateau strain, also known as the superelastic strain in micropillars with sizes of 2800nm, 2300nm, 1900nm and 1500nm, marked as ϵ_t in Figure 3 showing an increasing the transformation stress. The superelastic strains for these micro-sized pillars were measured as 0.2 ~ 0.3%. To verify whether measured superelastic strain is caused by the formation of transformation twins, we examined the crystallographic

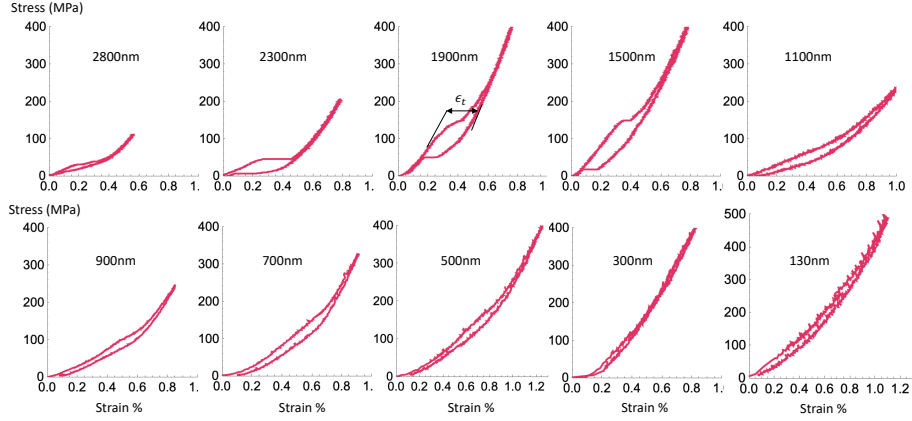


Figure 3: Stress-strain behaviors to reveal the superelasticity at sizes from 150nm to 3000nm.

equations for the twin laminate ($\mathbf{U}_1, \mathbf{U}_2$) as

$$\mathbf{Q}\mathbf{U}_2 = \mathbf{U}_1 + \mathbf{a} \otimes \mathbf{n} \quad (4)$$

$$\mathbf{R}(\mathbf{U}_1 + f\mathbf{a} \otimes \mathbf{n}) = \mathbf{I} + \mathbf{b} \otimes \mathbf{m}, \quad (5)$$

where \mathbf{n} specifies the twinning plane and \mathbf{a} determines the relative shear of variant \mathbf{U}_1 with respect to \mathbf{U}_2 . Rotation matrices \mathbf{Q} and $\mathbf{R} \in SO(3)$ rotate the deformed configurations to fit the reference lattice, along the habit plane normal \mathbf{m} and relative shear $\mathbf{b} \in \mathbb{R}^3$ with twinning volume fraction $f \in [0, 1]$. Strictly speaking, the exact solutions of $(f, \mathbf{b}, \mathbf{m})$ are not attained for neither twin systems given by the lattice parameters of BaTiO_3 , as the middle eigenvalue μ_2 of the tensor $\mathbf{C}_f = (\mathbf{U}_1 + f\mathbf{n} \otimes \mathbf{a})(\mathbf{U}_1 + f\mathbf{a} \otimes \mathbf{n})$ is not 1 for any value of the twinning volume fraction $f \in [0, 1]$, illustrated in Figure 4(a). The minimal distance between μ_2 and 1 is at the volume fraction $f = 0.5$, corresponding to $|\mu_2(0.5) - 1| = 0.0065$. Physically, this measures the middle principle eigenstrain of the phase transformation in the weak sense [36].

The characteristic equation

$$g(f) = \det(\mathbf{C}_f - \mathbf{I}) = 0, \quad (6)$$

does not have real-value roots of $f \in [0, 1]$ for the given \mathbf{U}_1 in (1). This is elaborated in Figure 4(b). Based on the geometrically nonlinear theory of martensite[36], the twins comprised of the pair of variants ($\mathbf{U}_1, \mathbf{U}_2$) are not exactly compatible with the tetragonal lattice. The volumetric measure of the misfit between the twinned martensite and austenite at the interface is estimated by $|g(f)|$. If the misfit can be compensated by localized plastic deformation, the formation of a pseudocompatible twin is possible. In this case, we can find an ansatz for $\mathbf{n} = (0, 0, -1)$ and $\mathbf{a} = \eta(-0.9999, 0, 0.0013)$ with shear $\eta = 0.0053$, which approximately

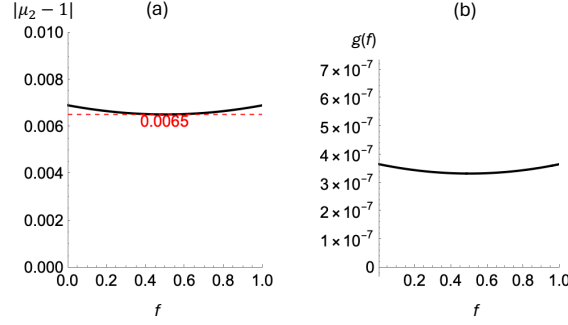


Figure 4: (a) The measure of compatibility of twins. (b) The characteristic polynomial for the formation of pseudo-compatible twins.

solves the equation (5). We have $\min |g(f)| = |g(0.5)| = 3.34 \times 10^{-7}$ corresponding to the solution for

$$\text{plane normal: } \mathbf{m} = (0.787, 0, -0.617) \quad (7)$$

$$\text{shear vector: } \mathbf{b} = (0.0067, 0, 0.0053) \quad (8)$$

with twinning volume fraction $f = 0.5$. It implies that the orthorhombic twin laminates are pseudo-compatible with austenite, corresponding to sufficiently small $|g(0.5)|$. Under the compression, the localized plastic strain field may drive the formation of pseudo-compatible twins due to the strain gradient. The stress-induced transformation strain can be directly calculated as a function of the loading direction \mathbf{N}

$$\epsilon_{\text{cal}}(\mathbf{N}) = \sqrt{\mathbf{N} \cdot \mathbf{N} + 2(\mathbf{m} \cdot \mathbf{N})(\mathbf{b} \cdot \mathbf{N}) + (\mathbf{b} \cdot \mathbf{b})(\mathbf{m} \cdot \mathbf{N})^2} - \mathbf{N} \cdot \mathbf{N}. \quad (9)$$

In our experiment, $\mathbf{N} = (0.041, 0.91, -0.411)$, that gives the transformation strain $\epsilon_{\text{cal}} = -0.00254$, which agrees very well with the measured superelastic strains, denoted as ϵ_t in Figure 3 for pillars larger than $1 \mu\text{m}$.

At a moderate stress level (i.e. $\sim 400 \text{MPa}$), the stress-strain behaviors for nanopillars smaller than $1 \mu\text{m}$ become nonlinear without a clear superelastic plateau. The nonlinear elastic behavior as well as about 1% recoverable strains were characterized for these small nanopillars. As the size of the pillar decreases, the stress hysteresis gradually diminishes, and the superelastic feature becomes less pronounced.

3.2. Size dependent strength of BaTiO_3 nanopillars

We increased the maximum compression stress beyond 400MPa to observe the plastic deformation and fracture in BaTiO_3 pillars with sizes varying from 100nm to 3000nm . We conducted a series of nanomechanical compression tests under the displacement control. An escalating series of maximum displacements were systematically applied to load and unload the nanopillars until the point of fracture. To ensure a quasi-static mechanical response, all tests were carried out at the strain rate of $0.1\%/s$. SEM figures of post-mortem nanopillars were taken to reveal the fracture microstructure.

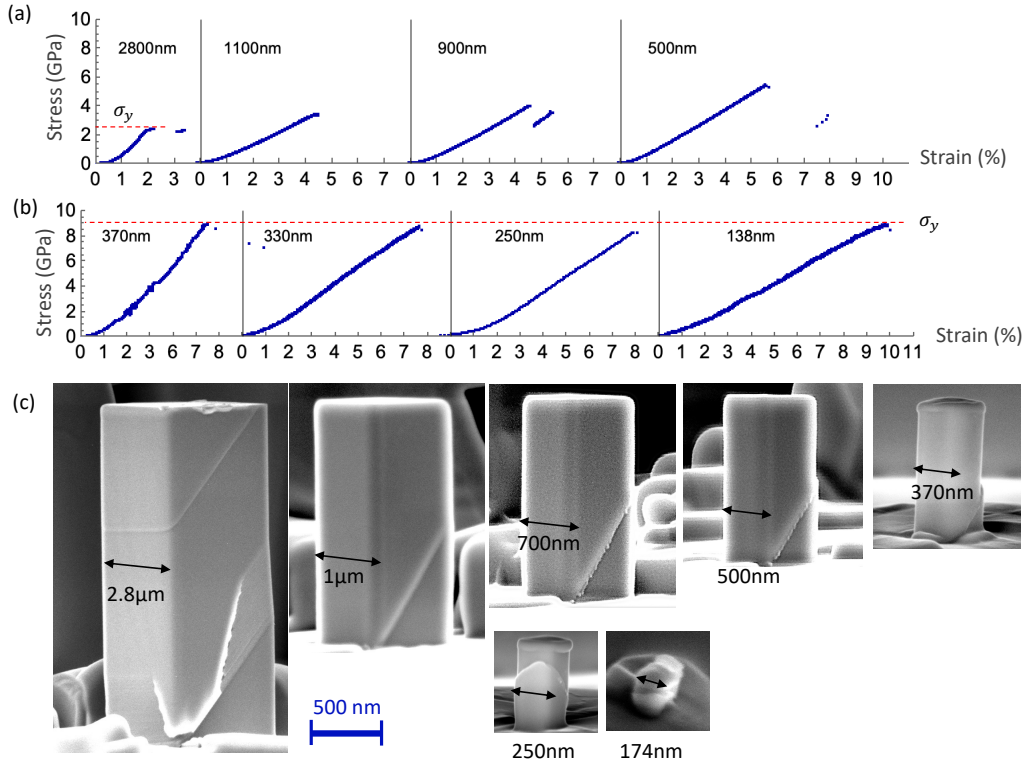


Figure 5: (a) Stress-strain curves for typical bulk sized pillars. (b) Stress-strain curves for nanopillars near and below the critical size. (c) The fracture microstructure of BaTiO_3 nanopillars from 100nm to 3000nm sizes.

The yield strength, denoted as σ_y , is characterized as the flow stress right before the fracture point of tested nanopillars, as seen in Figure 5(a). Here a representative micron-sized pillar (2800nm) yields at 2.5GPa with 2% overall strains. As the size reduces, there exist a clear trend of strengthening effect among pillars with sizes of 2800nm, 1100nm, 900nm and 500nm. In contrast, the strengthening effect was saturated for nanopillars with sizes of 370nm, 330nm, 250nm, 174nm respectively. Figure 5(b) shows that these small nanopillars yield at around 8.5GPa stress with 7% to 10% overall strains. The microstructure at the yield point of tested nanopillars were presented in Figure 5(c). For large pillars (i.e. $> 1\mu\text{m}$), both slips and twins were seen on lateral surfaces, while only slips were observed in small pillars (i.e. $< 1\mu\text{m}$).

4. Discussion

4.1. Scaling law, twins and slips in BaTiO_3 pillars over 330nm

We have systematically tested over 20 nanopillars with size homogeneously distributed in a range from 3000nm to 100nm. Figure 6 shows the size dependent yield strength with a power law fitting. Unlike the

typical presence of size effect reported in metals and alloys [27, 28], the strength of BaTiO₃ nanopillars does not increase as further reduction of size below 330nm. All nanopillars with size smaller than 330nm exhibit the same yield strength, around 9GPa, that approaches to the theoretical strength of BaTiO₃ [11], estimated by one tenth of the elastic modulus based on the Griffith theory of fracture[37, 38]. Our experiment revealed the existence of a critical size at 330nm in BaTiO₃ phase-transforming ferroelectric oxide. Above it, the size effect plays an important role. Below it, the material uniformly reaches its theoretical strength. **Similar phenomenon was reported in molybdenum (a bcc crystal) that the theoretical strength, i.e. approximately 9GPa, was achieved in nanopillars with sizes 360nm, 500nm, 750nm and 1000nm under the uniaxial compression tests.**[39] Noted that 330nm is not a considerably small length scale. The grains with 300 ~ 400nm sizes in polycrystals can be easily achieved by ordinary material synthesis techniques.

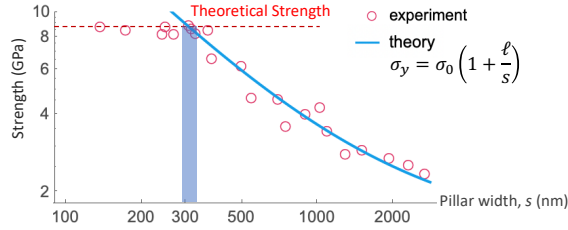


Figure 6: Size dependent yield strength of BaTiO₃ pillars from 100nm to 3000nm. The red dashed line marks the theoretical strength predicted by $E/10$, where E is the elastic modulus of BaTiO₃. σ_0 is the size-independent yield stress and ℓ is the material length parameter related to the strain-gradient hardening effect.

Phenomenologically, the phase-transforming material also follows a trend that gets stronger as the size reduces [40]. The size effect is often interpreted as the starving of defects in small scales [28] and geometrically necessity of defect mobility [26, 22]. For non-transforming metallic single crystal, plastic strain hardening is a common strengthening mechanism, but not responsible for the size effect. Mechanism-based models studied the size effect based on the strain-gradient theories [22, 41], considering the geometrically necessary dislocations (ρ_G) as a consequence of the gradient field of plastic strain (γ), symbolically presented as $\rho_G \sim \frac{1}{b} |\frac{\partial \gamma}{\partial x}|$ where b denotes the Burgers vector along x -axis. A general contribution of plastic strain gradient to the free energy density (ψ_g) follows a power law as $\psi_g \sim |\ell \frac{\partial \gamma}{\partial x}|^{p+1}$ where ℓ is a constitutive length parameter. The exponent p is an integer, depending on the order of nonlocal energy growth [41]. For a single crystal bending test, the length parameter represents the mean spacing between geometrically necessary dislocations. In other mechanical tests, this parameter is related to an internal material length scale responsible for size-dependent hardening effect. Strain gradient models predicted the yielding condition with an effective flow stress

$$\sigma_y = \sigma_0 \left[1 + \left(\frac{\ell}{s} \right)^\alpha \right], \quad (10)$$

where s denotes the effective size measure of plastic deformation domain, σ_0 is the size-independent yield

stress and α is the scaling exponent. Under the assumptions of rigid-plastic and linear deformation, the scaling exponent α with a value of 1 is found to be a non-trivial minimizer of the free energy [41]. Contrarily, experimental data from common metals and alloys [42, 43] typically show a scaling exponent close to 0.5, a phenomenon known as the Hall-Petch rule. In the case of certain body-centered cubic (bcc) and face-centered cubic (fcc) metals, the experimental scaling exponent ranges between 0.2 and 0.7 [25, 26, 27, 28]. By far, there is no experimental evidence that indicates the scaling exponent, α asymptotically converging to an exact value of 1.

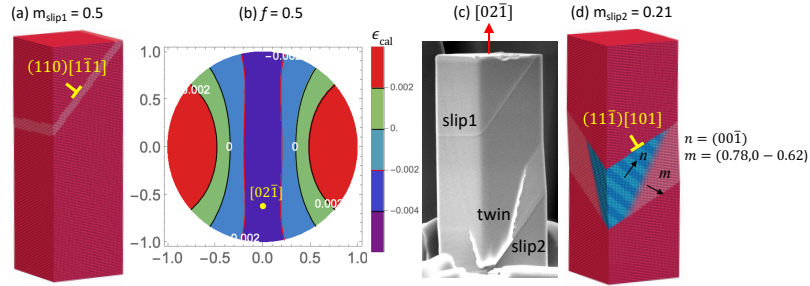


Figure 7: Microstructure of the post deformed micro pillar for micropillar. (a) Theoretical calculation of the slip system 1 (110)[111] corresponding to the maximum Schmid factor $m_{\text{slip1}} = 0.5$. (b) Stereographic contours of transformation strain ϵ_{cal} . (c) The post-mortem image of the 2800nm micropillar after fracture. (d) Theoretical calculation of the twin laminates within the slip band (111)[101] corresponding to a smaller Schmid factor $m_{\text{slip2}} = 0.21$.

We use the model in (10) to fit the experimental data for pillar sizes greater than the critical size (330nm), shown in Figure 6. Strikingly, we obtained the scaling exponent $\alpha = 0.999993$ (i.e. identical to 1) with $\sigma_0 = 1.3662\text{GPa}$ and material length parameter $\ell = 1670.37\text{nm}$. Figure 6 shows that the theory given in (10) with $\alpha = 1$ agrees very well with the size-dependent yield strength of BaTiO_3 with sizes greater than 330nm. We use Nix and Gao's model [22] to estimate the Burgers vector of the geometrically necessary dislocations as $b \approx \ell \left(\frac{\sigma_0}{G}\right)^2 = 6.36\text{\AA}$ for shear modulus $G \sim 70\text{GPa}$ [44]. With given lattice parameters of the tetragonal BaTiO_3 , the estimated magnitude of Burgers vector match the slip along $[1\bar{1}1]$ on (101) plane very well. The Schmid factor of (110)[111] system with respect to the loading direction $\mathbf{N} = (0.041, 0.91, -0.411)$ is calculated as $m_{\text{slip1}} = 0.5$. Figure 7(a) shows the calculated microstructure of the surface step due to (110)[111] slip, confirmed by the observed surface microstructure in the post-mortem image of the 2800nm micropillar as seen in Figure 7(c). Besides the activation of slip system with a high Schmid factor, we observed a wide surface step in the middle part of the same cuboidal micropillar, which suggests a different deformation mechanism.

The stereographic contours of the orientation-dependent transformation strain, denoted as ϵ_{cal} , were computed by (9), illustrated in Figure 7(b). The pillar orientation, characterized as $\mathbf{N} \sim [02\bar{1}]$, corresponds to a transformation strain ranging from 0.2% to 0.4%. The strain prior to the first burst of the 2800nm

pillar, as measured in Figure 5(a), allows us to estimate a plastic strain of approximately $1.6 \sim 1.8\%$ at a stress level of 2.5GPa. A comparison with the surface steps, captured in the post-mortem image of plastically deformed micropillar, leads us to hypothesize the formation of a pseudo-compatible twin within a plastic domain associated with a distinct slip system. Among the possible slip systems discussed in section 2 and as plotted in Figure 1, we identify the $(11\bar{1})[101]$ slip system that agrees with the experimental observation in Figure 7(c). Although $(11\bar{1})[101]$ slip corresponds to a low Schmid factor ($m_{\text{slip}2} = 0.21$), it is facilitated by the formation of pseudocompatible twins during compression-induced transformation.

4.2. Size-independency of BaTiO_3 nanopillars smaller than critical size

At 330nm, the yield strength of BaTiO_3 nanopillar reaches a saturation value, i.e. the theoretical strength, near 9GPa. The size effect is no longer observed in the nanopillars smaller than 330nm. The stress-strain curves of nanopillars with sizes from 100nm to 300nm are shown in Figure 5(b), exhibiting $8 \sim 10\%$ plastic strains. As a comparison, the β -titanium alloy fractures with 8% strain under 1.4GPa compressive stress [45]. Stainless steels have even less plastic strains.

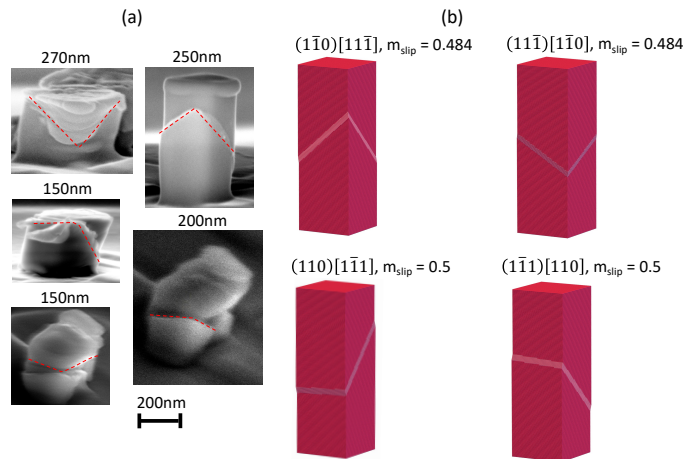


Figure 8: (a) Microstructure of plastically deformed nanopillars with a single slip system and duplex slip systems. (b) Theoretical calculations of possible slip systems for nanopillars in the size-independent regime.

More size-independent experimental data is verified in Figure 6, plateaued at the theoretical strength of BaTiO_3 . Figure 8(a) shows the post-mortem image of the nanopillars below the critical size. We did not observe any twins or twin-like morphology in these nanopillars, indicating that the stress-induced transformation is suppressed at this scale. Only a single slip or duplex slips were observed, corresponding to the slip systems with high Schmid factors as illustrated in Figure 8(b). Note that these slip systems consist of the conventional close-packed planes and directions of body-center and face-center cubic lattices, which are rarely reported in BaTiO_3 ferroelectric materials.

A recent strain-gradient theory [41] considers both linear and superlinear growth of nonlocal strain-gradient energy. Direct energy minimization yields a scaling exponent $\alpha = 1$ for ideal plasticity with linear energy growth, while size dependency of strain-gradient energy disappears for superlinear growth. The size-independent strength of BaTiO₃ nanopillars ($< 330\text{nm}$) suggests that plastic deformation, reaching the theoretical strength, is driven by superlinear growth of nonlocal strain-gradient energy. The multi-slips of $(1\bar{1}0)[11\bar{1}]$, $(1\bar{1}1)[110]$, $(110)[1\bar{1}1]$, $(1\bar{1}1)[110]$ and their crystallographic equivalencies, are completely inert to plastic hardening until the external stress reaching the theoretical strength limit. However, the critical size of 300nm can not be quantitatively related to the nonlocal strain gradient theory as the statistically stored dislocation density is not available.

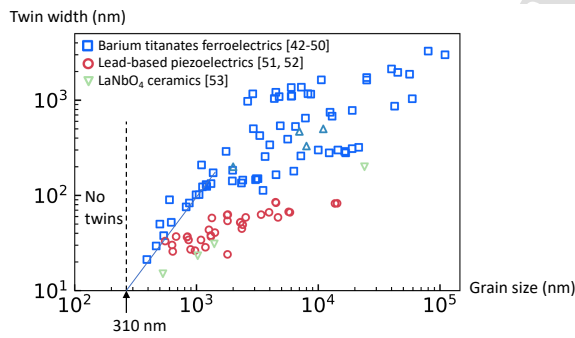


Figure 9: Size correlation between average twin width and mean grain size of Barium titanates, lead-based piezoelectrics and LaNbO₄ ceramics reported in literature.

As shown in Figure 9, we summarized the size correlation between the average twin width and mean grain size of Barium titanates [46, 47, 48, 49, 50, 51, 52, 53, 54], Lead-based piezoelectrics [55, 56], and LaNbO₄ ceramics [57]. The plotted twin width was determined directly from the microstructure images reported in the literature on polycrystalline ferroelectrics. The measurements are not influenced by internal strain or orientation of the grains. We calculated the twin width by taking the average of the widths of many twins observed across different grains. Similarly, the grain size was determined by averaging the sizes of the grains visible in the micrographs. Twins can be observed in the grain with size larger than 310nm . The twin gets finer as the grain size reduces. In phase-transforming ferroelectrics, we revealed that a universal critical grain size exists, below which no twins were observed in experiments. This critical size is consistent with the critical size we discovered in Figure 6.

5. Conclusion

In this paper, we systematically studied the stress-induced martensitic transformation (i.e. superelasticity) and plastic deformation in BaTiO₃ nanopillars with size varying from 3000nm to 100nm . At low-level

stress ($< 400\text{MPa}$), the nanopillars exhibit superelasticity, which is characterized by a reversible phase transformation. We used the crystallographic theory of martensite to precisely predict the transformation strains that agree well with the measured superelastic strains for pillars greater than $1\mu\text{m}$. The superelasticity is associated with the formation of pseudocompatible twins, which are driven by the localized plastic condition. In addition, we characterized the size-dependent yield strength of BaTiO_3 nanopillars at a high-level stress ($> 2\text{GPa}$). We found a critical size at 330nm . Above this size, the yield strength is size dependent, growing with an exactly scaling exponent $\alpha = 1$. Below the critical size, the yield strength reaches the theoretical strength of BaTiO_3 , near 9GPa , and becomes size independent. The size-independent strength is driven by superlinear growth of nonlocal strain-gradient energy. The multi-slips of $(1\bar{1}0)[11\bar{1}]$, $(1\bar{1}1)[110]$, $(110)[1\bar{1}1]$, $(1\bar{1}1)[110]$ and their crystallographic equivalencies, are completely inert to plastic hardening until the external stress reaching the theoretical strength limit. The size-independent strength of BaTiO_3 nanopillars is consistent with the critical grain size below which no twins were observed in experiments.

6. Acknowledgment

Z.Z., M. K, K.H.C., and X.C. thank the financial support under GRF Grants No. 16203021, 16204022 and No. 16203023 by Research Grants Council, Hong Kong, and ITF Seed Grant No. ITS/354/21 by Innovation and Technology Commission, HK. C. Z. thanks the support by National Natural Science Foundation of China (No.12204350), Fundamental Research Funds for the Central Universities (No.22120240009).

References

- [1] H. Huang, J. F. Scott, *Ferroelectric materials for energy applications*, John Wiley & Sons, 2018.
- [2] A. Erturk, D. J. Inman, *Piezoelectric energy harvesting*, John Wiley & Sons, 2011.
- [3] Y. Wang, Z. Zhang, T. Usui, M. Benedict, S. Hirose, J. Lee, J. Kalb, D. Schwartz, A high-performance solid-state electrocaloric cooling system, *Science* 370 (6512) (2020) 129–133.
- [4] C. Zhang, Y. Song, M. Wegner, E. Quandt, X. Chen, Power-source-free analysis of pyroelectric energy conversion, *Phys. Rev. Appl.* 12 (2019) 014063.
- [5] C. Zhang, Z. Zhu, J. Y. Choi, J. Y. Kim, X. Chen, Low hysteresis and enhanced figure-of-merit of pyroelectric energy conversion at compatible phase transformation, *Applied Physics Letters* 119 (8) (2021).
- [6] G. Kwei, A. Lawson, S. Billinge, S. Cheong, Structures of the ferroelectric phases of barium titanate, *The Journal of Physical Chemistry* 97 (10) (1993) 2368–2377.
- [7] R. Zeches, M. Rossell, J. Zhang, A. Hatt, Q. He, C.-H. Yang, A. Kumar, C. Wang, A. Melville, C. Adamo, et al., A strain-driven morphotropic phase boundary in BiFeO_3 , *science* 326 (5955) (2009) 977–980.
- [8] A. Reichmann, S. Mitsche, A. Zankel, P. Pölt, K. Reichmann, In situ mechanical compression of polycrystalline BaTiO_3 in the esem, *Journal of the European Ceramic Society* 34 (10) (2014) 2211–2215.
- [9] F. H. Schader, N. Khakpash, G. A. Rossetti, K. G. Webber, Phase transitions in BaTiO_3 under uniaxial compressive stress: Experiments and phenomenological analysis, *Journal of Applied Physics* 121 (6) (2017).
- [10] A. Reichmann, S. Mitsche, A. Zankel, P. Pölt, K. Reichmann, In situ mechanical compression of polycrystalline BaTiO_3 in the esem, *Journal of the European Ceramic Society* 34 (10) (2014) 2211–2215.

- [11] R. C. Pohanka, S. W. Freiman, B. Bender, Effect of the phase transformation on the fracture behavior of batio₃, *Journal of the American Ceramic Society* 61 (1-2) (1978) 72–75.
- [12] N. G. Mathews, A. K. Saxena, C. Kirchlechner, G. Dehm, B. N. Jaya, Effect of size and domain orientation on strength of barium titanate, *Scripta Materialia* 182 (2020) 68–73.
- [13] D. Liu, M. Chelf, K. White, Indentation plasticity of barium titanate single crystals: Dislocation influence on ferroelectric domain walls, *Acta materialia* 54 (17) (2006) 4525–4531.
- [14] T. Scholz, K. McLaughlin, F. Giuliani, W. Clegg, F. Espinoza-Beltrán, M. Swain, G. Schneider, Nanoindentation initiated dislocations in barium titanate (ba ti o₃), *Applied Physics Letters* 91 (6) (2007) 062903.
- [15] Y. Gaillard, A. H. Macías, J. Muñoz-Saldaña, M. Anglada, G. Trápaga, Nanoindentation of BaTiO₃: dislocation nucleation and mechanical twinning, *Journal of Physics D: Applied Physics* 42 (8) (2009) 085502.
- [16] N. Doukhan, J. Doukhan, Dislocations in perovskites batio₃ and catio₃, *Physics and chemistry of minerals* 13 (6) (1986) 403–410.
- [17] O. Eibl, P. Pongratz, P. Skalicky, H. Schmelz, Dislocations in BaTiO₃ ceramics, *Physica status solidi (a)* 108 (2) (1988) 495–502.
- [18] K. Chu, Y. Li, X. Wang, Z. Wu, Q. Peng, J. Li, L.-Q. Chen, F. Ren, Q. Sun, Superelastic ferroelectric micropillar with large hysteresis and super-durability, *Acta Materialia* 258 (2023) 119140.
- [19] Y. Li, K. Chu, C. Liu, P. Jiang, K. Qu, P. Gao, J. Wang, F. Ren, Q. Sun, L. Chen, et al., Superelastic oxide micropillars enabled by surface tension–modulated 90° domain switching with excellent fatigue resistance, *Proceedings of the National Academy of Sciences* 118 (24) (2021) e2025255118.
- [20] E. Hall, The deformation and ageing of mild steel: Ii characteristics of the lüders deformation, *Proceedings of the physical society. Section B* 64 (9) (1951) 742.
- [21] N. Hansen, Hall–petch relation and boundary strengthening, *Scripta materialia* 51 (8) (2004) 801–806.
- [22] H. Gao, Y. Huang, W. D. Nix, J. W. Hutchinson, Mechanism-based strain gradient plasticity—i. theory, *Journal of the Mechanics and Physics of Solids* 47 (6) (1999) 1239–1263.
- [23] M. E. Gurtin, A gradient theory of single-crystal viscoplasticity that accounts for geometrically necessary dislocations, *Journal of the Mechanics and Physics of Solids* 50 (1) (2002) 5–32.
- [24] P. Gudmundson, A unified treatment of strain gradient plasticity, *Journal of the Mechanics and Physics of Solids* 52 (6) (2004) 1379–1406.
- [25] Y. Mu, K. Chen, W. Meng, Thickness dependence of flow stress of cu thin films in confined shear plastic flow, *MRS Communications* 4 (3) (2014) 129–133.
- [26] Y. Mu, X. Zhang, J. Hutchinson, W. Meng, Dependence of confined plastic flow of polycrystalline cu thin films on microstructure, *MRS Communications* 6 (3) (2016) 289–294.
- [27] J.-Y. Kim, D. Jang, J. R. Greer, Tensile and compressive behavior of tungsten, molybdenum, tantalum and niobium at the nanoscale, *Acta Materialia* 58 (7) (2010) 2355–2363.
- [28] J. R. Greer, W. C. Oliver, W. D. Nix, Size dependence of mechanical properties of gold at the micron scale in the absence of strain gradients, *Acta Materialia* 53 (6) (2005) 1821–1830.
- [29] R. Rhodes, Barium titanate twinning at low temperatures, *Acta Crystallographica* 4 (2) (1951) 105–110.
- [30] J. Harada, T. Pedersen, Z. Barnea, X-ray and neutron diffraction study of tetragonal barium titanate, *Acta Crystallographica Section A: Crystal Physics, Diffraction, Theoretical and General Crystallography* 26 (3) (1970) 336–344.
- [31] X. Chen, V. Srivastava, V. Dabade, R. D. James, Study of the cofactor conditions: conditions of supercompatibility between phases, *Journal of the Mechanics and Physics of Solids* 61 (12) (2013) 2566–2587.
- [32] A. Beauger, J. Mutin, J. Niepce, Synthesis reaction of metatitanate BaTiO₃: Part 2 study of solid-solid reaction interfaces, *Journal of materials science* 18 (1983) 3543–3550.

- [33] C. Zhang, Z. Zhu, K. H. Chan, R. Huang, X. Chen, Enhanced functional reversibility in lead-free ferroelectric material over long cycle pyroelectric energy conversion, *Phys. Rev. Mater.* 7 (2023) 064408.
- [34] M. Karami, K. Chu, Z. Zhu, Z. Wang, Q. Sun, M. Huang, X. Chen, Orientation-dependent superelasticity and fatigue of CuAlNi alloy under in situ micromechanical tensile characterization, *Journal of the Mechanics and Physics of Solids* 160 (2022) 104787.
- [35] M. Karami, Z. Zhu, K. H. Chan, P. Hua, N. Tamura, X. Chen, Nondissipative martensitic phase transformation after multimillion superelastic cycles, *Physical Review Letters* 132 (6) (2024) 066101.
- [36] J. M. Ball, R. D. James, Fine phase mixtures as minimizers of energy, *Archive for Rational Mechanics and Analysis* 100 (1987) 13–52.
- [37] A. A. Griffith, Vi. the phenomena of rupture and flow in solids, *Philosophical transactions of the royal society of london. Series A, containing papers of a mathematical or physical character* 221 (582-593) (1921) 163–198.
- [38] E. Orowan, Fracture and strength of solids, *Reports on progress in physics* 12 (1) (1949) 185.
- [39] H. Bei, S. Shim, E. P. George, M. K. Miller, E. Herbert, G. M. Pharr, Compressive strengths of molybdenum alloy micro-pillars prepared using a new technique, *Scripta materialia* 57 (5) (2007) 397–400.
- [40] M. Karami, X. Chen, Nanomechanics of shape memory alloys, *Materials Today Advances* 10 (2021) 100141.
- [41] C. F. Dahlberg, M. Ortiz, Fractional strain-gradient plasticity, *European Journal of Mechanics-A/Solids* 75 (2019) 348–354.
- [42] D. Dunstan, A. Bushby, Grain size dependence of the strength of metals: The hall–petch effect does not scale as the inverse square root of grain size, *International Journal of Plasticity* 53 (2014) 56–65.
- [43] B. Ehrler, X. Hou, T. Zhu, K. P'ng, C. J. Walker, A. Bushby, D. J. Dunstan, Grain size and sample size interact to determine strength in a soft metal, *Philosophical Magazine* 88 (25) (2008) 3043–3050.
- [44] G. J. Fischer, Z. Wang, S.-i. Karato, Elasticity of CaTiO_3 , SrTiO_3 and BaTiO_3 perovskites up to 3.0 gpa: the effect of crystallographic structure, *Physics and Chemistry of Minerals* 20 (1993) 97–103.
- [45] W. Q. Song, S. Sun, S. Zhu, G. Wang, J. Wang, M. S. Dargusch, Compressive deformation behavior of a near-beta titanium alloy, *Materials & Design* 34 (2012) 739–745.
- [46] D. Ghosh, A. Sakata, J. Carter, P. A. Thomas, H. Han, J. C. Nino, J. L. Jones, Domain wall displacement is the origin of superior permittivity and piezoelectricity in BaTiO_3 at intermediate grain sizes, *Advanced Functional Materials* 24 (7) (2014) 885–896.
- [47] H.-I. Hsiang, F.-S. Yen, Effect of crystallite size on the ferroelectric domain growth of ultrafine BaTiO_3 powders, *Journal of the American Ceramic Society* 79 (4) (1996) 1053–1060.
- [48] P. Zheng, J. Zhang, Y. Tan, C. Wang, Grain-size effects on dielectric and piezoelectric properties of poled BaTiO_3 ceramics, *Acta Materialia* 60 (13-14) (2012) 5022–5030.
- [49] T. Hoshina, K. Takizawa, J. Li, T. Kasama, H. Kakemoto, T. Tsurumi, Domain size effect on dielectric properties of barium titanate ceramics, *Japanese Journal of Applied Physics* 47 (9S) (2008) 7607.
- [50] T. Hoshina, Y. Kigoshi, S. Hatta, H. Takeda, T. Tsurumi, Domain contribution to dielectric properties of fine-grained BaTiO_3 ceramics, *Japanese Journal of Applied Physics* 48 (9S1) (2009) 09KC01.
- [51] G. Arlt, P. Sasko, Domain configuration and equilibrium size of domains in BaTiO_3 ceramics, *Journal of Applied Physics* 51 (9) (1980) 4956–4960.
- [52] N. Ma, B.-P. Zhang, W.-G. Yang, D. Guo, Phase structure and nano-domain in high performance of BaTiO_3 piezoelectric ceramics, *Journal of the European Ceramic Society* 32 (5) (2012) 1059–1066.
- [53] G. Arlt, Twinning in ferroelectric and ferroelastic ceramics: stress relief, *Journal of materials Science* 25 (1990) 2655–2666.
- [54] Y. Huan, X. Wang, J. Fang, L. Li, Grain size effects on piezoelectric properties and domain structure of BaTiO_3 ceramics prepared by two-step sintering, *Journal of the American Ceramic Society* 96 (11) (2013) 3369–3371.
- [55] W. Cao, C. A. Randall, Grain size and domain size relations in bulk ceramic ferroelectric materials, *Journal of Physics*

- and Chemistry of Solids 57 (10) (1996) 1499–1505.
- [56] G. Picht, N. H. Khansur, K. G. Webber, H. Kungl, M. J. Hoffmann, M. Hinterstein, Grain size effects in donor doped lead zirconate titanate ceramics, Journal of applied physics 128 (21) (2020).
- [57] S. Tsunekawa, H. Takei, Domain switching behaviour of ferroelastic lanbo4 and ndnbo4, Journal of the Physical Society of Japan 40 (5) (1976) 1523–1524.

Journal Pre-proof

Statement of Novelty (To the best of your knowledge, does any existing work (either submitted or already published, including your

Statement of novelty

The authors of the manuscript titled "Twinning, Slip and Size Effect of Phase-Transforming Ferroelectric Nanopillars" declare the following:

To the best of our knowledge, all existing work done in this paper is original, which has not been published or under consideration of publishing by any other journals.

This declaration of interest statement is provided to ensure the transparency and integrity of our research, and to adhere to the guidelines provided by Elsevier.

Xian Chen,
Mechanical and Aerospace Engineering
The Hong Kong University of Science and Technology

AUTHOR STATEMENT

Manuscript title: Twinning, Slip and Size Effect of Phase-Transforming Ferroelectric Nanopillars

All persons who meet authorship criteria are listed as authors, and all authors certify that they have participated in the work to take public responsibilities for the content including participation of concept, design, analysis, writing, or revision of the manuscript. Furthermore, each author certifies that this material is has not been and will not be submitted to or published in any other publication before its appearance in the Journal of the Mechanics and Physics of Solids.

Authorship contributions

First author: Zeyuan Zhu

Designed and conducted major experiments including FIB fabrication of nanopillars with varying sizes, nanomechanical characterization, microstructure characterization. Analyzed the data and wrote the paper.

Co-author: Mostafa Karami

Design and assist in situ nanomechanical experiments, contributing to the data interpretation and discussion of the paper contents.

Co-author: Chenbo Zhang

Synthesis of the high quality phase-transforming ferroelectric oxides with coarse grains. Participation of structural characterization, data analysis and paper writing.

Corresponding author: Xian Chen

Design the research framework and formulate the problem. Analyzed the results and interpreted primary finds and wrote the majority of the manuscript.

Acknowledgements

All persons who have made substantial contributions to the work reported in the manuscript are named in the Acknowledgement and have given us their written permission to be named in the manuscript. This statement is signed by all the authors

<u>Author Name</u>	<u>Signature</u>	<u>Date</u>
Zeyuan Zhu	<i>Zeyuan Zhu</i>	1 st June2024
Mostafa Karami	<i>m. Karami</i>	1 st June2024
Chenbo Zhang	<i>Chenbo Zhang</i>	1 st June2024
Xian Chen	<i>Xian Chen</i>	1 st June2024

Declaration of Interest

The authors of the manuscript titled "Twinning, Slip and Size Effect of Phase-Transforming Ferroelectric Nanopillars" declare the following:

1. On behalf of all of my co-authors, we declare that no conflict of interests in this paper.
2. To the best of our knowledge, all existing work done in this paper is original, which has not been published or under consideration of publishing by any other journals.

This declaration of interest statement is provided to ensure the transparency and integrity of our research, and to adhere to the guidelines provided by Elsevier.

Xian Chen,
Mechanical and Aerospace Engineering
The Hong Kong University of Science and Technology